# ACOUSTIC LAND FULL-WAVEFORM INVERSION WITH FREE-SURFACE TOPOGRAPHY IN OMAN

G. Royle[1], O. Leblanc[1], G. Viguier[1], G. Lambaré[1], A. Sedova[1], S. Shutova[1], D. Carotti[1]

[1] CGG

## Summary

Successful applications of full waveform inversion (FWI) to land datasets are far less numerous than marine applications, yet the development of dense, long-offset broadband acquisitions has presented promising opportunities. While challenges exist due to elastic effects, acoustic land FWI has been shown to provide accurate velocity models with a level of resolution traditionally seen only with marine data. The first successful land applications in Oman have been obtained on surveys with only minor variations in surface elevation, and have encouraged the development of FWI capabilities to handle more significant topography. We present a boundary-conforming free-surface topography method for FWI, cast in the curvilinear domain. In a synthetic example, we benchmark this approach against the use of an absorbing surface boundary and a replacement velocity in the air layer (the model extension method), and the method of applying statics shifts to compensate for elevation variations. Finally, we show two real data applications from North and South Oman where our free-surface topography tool illustrates imaging uplifts over FWI results obtained with an absorbing surface and legacy tomography.

## Introduction

While traditionally rare, land applications of FWI (Mei et al., 2014) are gaining momentum with the development of long-offset broadband acquisitions in the Middle East (Mahrooqi et al., 2012; Baeten et al., 2013). The first applications on such surveys were promising as they demonstrated that, in this context, FWI could be an efficient and accurate velocity building model tool (Stopin et al., 2014). Some difficulties associated with a lack of convergence at frequencies above 6 Hz were reported. This was attributed to potential elastic effects, and motivated investigations towards elastic land FWI (Perez-Solano and Plessix, 2019). Other studies, however, illustrate convergence of acoustic land FWI at higher frequencies using a workflow that incorporates dedicated data pre-processing and the introduction of reflected waves (Sedova et al., 2019). Such results were obtained on surveys with very mild elevation variations (residual variations were addressed by statics corrections), and interest now grows for the development of acoustic land FWI with surface topography (Huiskes et al., 2017).

A significant drawback of finite-difference (FD) methods is the difficulty in applying topography variations in a regularly-sampled numerical grid, and the associated increase in computational costs. Often the free-surface boundary condition is replaced by an absorbing boundary condition, and the velocity model is extended into the air using a replacement velocity (Tverdokhlebov et al., 2018; Vigh et al., 2018). We refer to this as the model extension method, which is significantly less expensive than applying irregular free-surface topography, although the reflection pheonomena associated with a free-surface will not be explained by updates to the velocity model. There are several irregular free-surface boundary methods, such as the vacuum method (Graves, 1996), the stress image method (Robertsson, 1996) and the boundary-conforming free-surface topography method (Zhang and Chan, 2006). In this last method, a conformal mapping operator aligns the numerical grid to the topography horizon so that the artefacts of a staircase surface boundary on a regularly-sampled grid are avoided.

In this paper, we present an acoustic land FWI tool based on the boundary-conforming free-surface topography method. We detail the associated FD modeling and show a synthetic experiment based on a modified 3D SEG/EAGE Overthrust model to benchmark three strategies: the boundary-conforming free-surface topography method, statics corrections with a flat surface boundary, and the model extension method. Finally, we show results obtained on two real data FWI studies from Oman demonstrating the capability of the method.

## Boundary-conforming free-surface topography method

Free-surface topography is implemented by mapping a rectangular auxiliary grid of $(\xi, \vartheta, \gamma)$-coordinates in the curvilinear domain into a curved grid in Cartesian $(x, y, z)$ coordinates using the flattening transform (Tessmer et al., 1992; Fornberg, 1988):

$$x(\xi, \vartheta, \gamma) = \xi; \quad y(\xi, \vartheta, \gamma) = \vartheta; \quad \text{and} \quad z(\xi, \vartheta, \gamma) = z_t(\xi, \vartheta) + \gamma \left[ 1 - \frac{z_t(\xi, \vartheta)}{z_{max}} \right]. \tag{1}$$

The parameter $z_t(\xi, \vartheta)$ defines the surface topography, which decays linearly with depth until reaching the maximum depth of the model $z_{max}$.
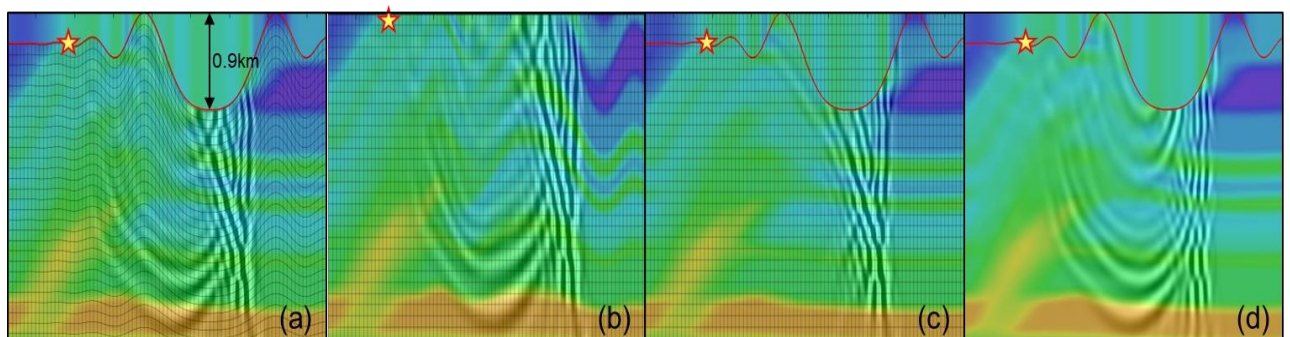


**Figure 1** *Wave propagation snapshots (1.4 s) superimposed on the velocity model and FD grids. The elevation variation is 900m. (a) free-surface topography implementation, (b) the wavefield cast in the regular curvilinear domain, (c) the model extension method and (d) the difference between (a) and (c).*

The curved grid in the *(x,y,z)*-domain is first calculated using the topography horizon and the flattening transform. The model parameters and survey acquisition are interpolated onto this curved grid. The wave propagation is computed on the auxiliary regular grid in $(\xi, \vartheta, \gamma)$ using first- and second-order spatial derivatives $\partial(\xi, \vartheta, \gamma)/\partial(x, y, z)$ and $\partial^2(\xi, \vartheta, \gamma)/\partial(x, y, z)^2$ as required in the 3D acoustic VTI wave equation (Zhang et al., 2011). Figure 1 shows the wavefield propagation with a free-surface at the topography horizon (a) versus a radiation condition obtained by vertically extending the velocity model above the horizon (the model extension method) shown in (c). Differences between the two wavefields (d) correspond to reverberations along the free-surface.

## Synthetic example

A synthetic FWI experiment using the SEG/EAGE 3D Overthrust model (Aminzadeh et al., 1997) is used to benchmark different approaches to surface topography. The "true" data are generated with our topography-conforming free-surface boundary condition. Despite the inverse crime, differences between results (Figure 2) obtained using free-surface topography, the model extension method, and data statics corrections provide insight into the benefits and drawbacks of each method. The elevation variation is approximately 600 m, and the initial model is a smoothed version of the true model. For the statics corrections method, a 3D linear regression is applied to the topography horizon producing a flat and sloping horizon $z_r$ (as done in Sedova et al., (2019b)). Statics corrections are applied to the data to account for the elevation differences between the topography $z_t$ and $z_r$. The initial velocity model for FWI is rotated to bring $z_r$ up to horizontal, and the final FWI result is re-rotated to recover the original $z_r$. No additional processing is applied to the "true" data to remove free-surface related phenomena.
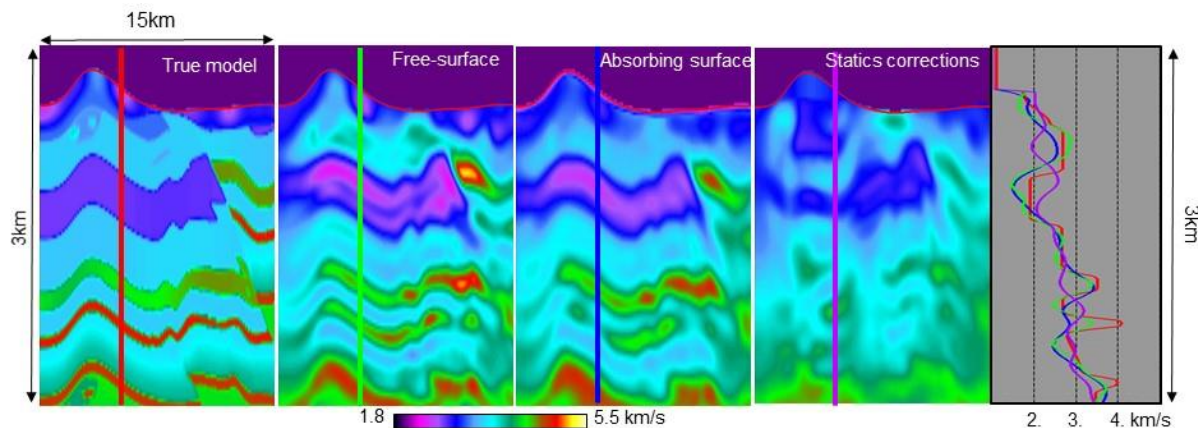


***Figure 2*** *The true and recovered FWI models for the synthetic SEG/EAGE 3D Overthrust FWI test. From left to right: the true velocity model, the FWI result using free-surface topography, the FWI result using the model extension method, the FWI result using flat topography and statics corrections, and finally, the velocity profiles for the four models at the location of the vertical line (red, green, blue and purple lines, respectively).*

The three methods provide similar results in regions where elevation variations are minimal. In regions with stronger topography, we observe a loss in structural integrity, the statics corrections approach in particular. The model extension method out-performs the statics corrections approach in terms of the delineating structures, particularly in the shallower part of the model, but this ideal case does not reach the quality and resolution obtained with free-surface topography (Figure 2).

## Real data applications

We apply our acoustic FWI with boundary-conforming free-surface topography to two Oman datasets. The first one is from the Block 62 in North Oman acquired by Oxy. Receiver lines are spaced 250 m, with 25 m between each receiver, and shots are spaced at 50 m intervals. The maximum offset is approximately 5.7 km. The topography has an elevation variation of 250 m. We compare the FWI results obtained using free-surface topography to those obtained using the model extension method (Figure 3). We observe improved event delineation, continuity and event flattening when using free-surface topography.
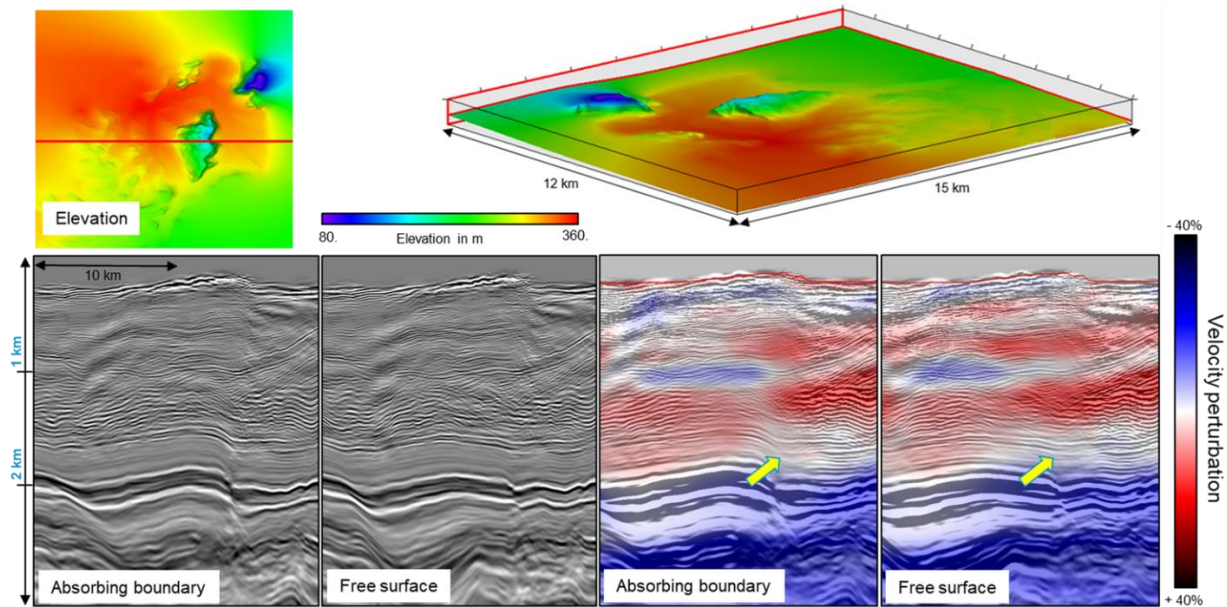
*Figure 3. Migrated stack images from OXY Block 62 (left), with the recovered model perturbation superimposed (right). Top: the elevation model. Bottom: migrated stacks (left) and velocity perturbation models (right) obtained with FWI using either free-surface topography or the model extension method. We see improvements in the focusing and continuity of the target zone: a shale package from approximately 1.5–2 km depth.*

The second application is from PDO and is located in South Oman, which is an area particularly challenging for imaging (due to very strong internal multiples) and acoustic FWI (due to elastic effects) (Perez Solano & Plessix, 2019)). Despite only gentle topography variations, using a free-surface boundary condition provides an improved result over using an absorbing boundary of partly modelled free-surface multiples. We observe on Figure 4 that the 8 Hz Optimal Transport (OT) FWI results (Messud and Sedova, 2019; Sedova et al., 2019a) obtained with boundary-conforming free-surface topography contain two major velocity inversions, which are well known difficulties in this area. The comparison with the legacy tomographic model shows that the 8 Hz OT-FWI nicely delineates these velocity variations (see the yellow ellipse).
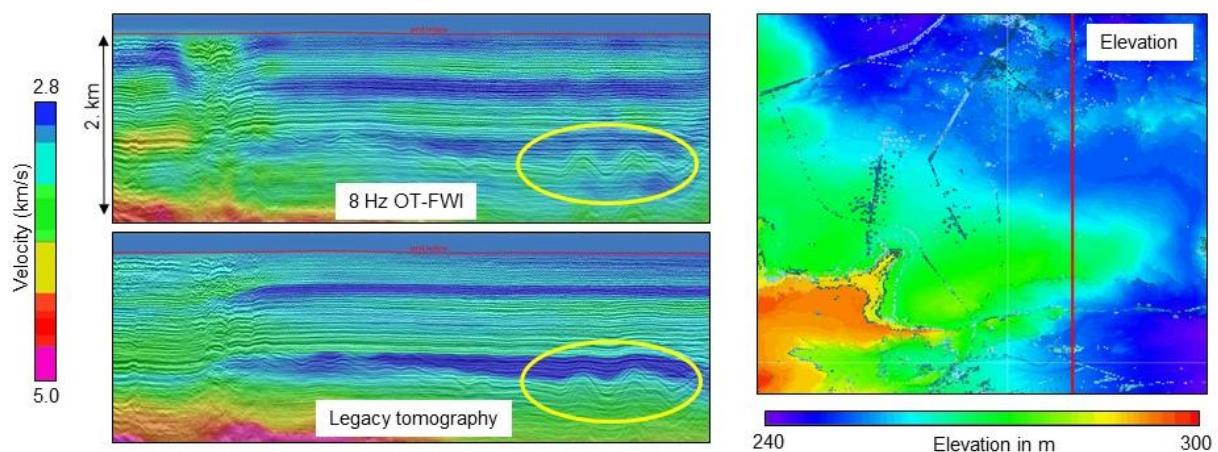


*Figure 4: Application of 8Hz acoustic OT- FWI to a broadband land dataset from South Oman. The elevation map shown on the right is quite gentle. On the left we observe the improved delineation of velocity structures (yellow ellipse) compared to the legacy tomography model (the location on the lines are indicated on the right by the red line).*

## Conclusions

We have developed and implemented a boundary-conforming free-surface topography method for acoustic land FWI, which allows us to simulate free-surface phenomena for land FWI in cases of elevation variations. A synthetic FWI example derived from the 3D SEG/EAGE Overthrust model (with

600 m of elevation variation) illustrates how this method outperforms both statics corrections and the model extension method. Applications to two land datasets from Oman illustrate the benefits of the approach in the context of mild elevation variations that characterize the Middle East.

## Acknowledgements

## References

Aminzadeh, F., Brac, J., and Kunz, T. [1997], 3-D salt and overthrust models: Soc. Expl. Geophy.

Baeten, G., ten Kroode, F., Rawahi, S. and Mahrooqi, S. [2013]. Onshore Low Frequency Acquisition for Full Waveform Inversion – from Field Trials to State of the Art Production Surveys. *75th EAGE Conference & Exhibition*, Extended abstract, I07.

Fornberg, B. [1988] The pseudospectral method: Accurate representation of interfaces in elastic wave calculations: *Geophysics*, **53**, 625-637.

Graves, R. W. [1996] Simulating seismic wave propagation in 3D elastic media using staggered-grid finite differences. *Bull. Seism. Soc. Am.,* **91**, 617-623.

Huiskes, M.J., R.E. Plessix, W.A. Mulder, 2017. Acoustic VTI Full-waveform Inversion with 3-D Free surface Topography, *79th EAGE Conference & Exhibition*, Extended abstract, Th A3 0.

Mahrooqi, S., S. Rawahi, S. Yarubi, S. Abri, A. Yahyai, M. Jahdhami, K. Hunt, and J. Shorter [2012] Land seismic low frequencies: Acquisition, processing and full wave inversion of 1.5-86 Hz: *82nd Annual International Meeting, SEG,* Expanded Abstracts, 1-5.

Mei, J., Ahmed, S., Searle, A. and Ting, C-O., [2014]. FWI Application on an Alaska Land 3D Survey. SEG Technical Program, Expanded Abstracts, 981-986.

Messud, J., Sedova, A. [2019] Multidimensional Optimal Transport for 3D FWI: Demonstration on Field Data. *81st EAGE Conference and Exhibition*, Extended abstract, Tu R08 02.

Perez Solano, C., R.E. Plessix [2019],Velocity-model building with enhanced shallow resolution using elastic waveform inversion – An example from onshore Oman: Geophysics, vol. 84, No. 6 (Nov-Dec 2019); P. R977-R988.

Robertsson, J. [1996] A numerical free-surface condition for elastic/viscoelastic finite-difference modeling in the presence of topography. *Geophysics*, **61**, 1921-1934.

Sedova, A., Messud, J., Prigent, H., Masclet, S., Royle, G., Lambaré, G. [2019a] Acoustic Land Full Waveform Inversion on a Broadband Land Dataset: the Impact of Optimal Transport. *81st EAGE Conference and Exhibition*, Extended abstract, Th R08 07.

Sedova A., G. Royle, T. Allemand, G. Lambaré and O. Hermant [2019b] High-frequency acoustic land full-waveform inversion: a case study from the Sultanate of Oman: *First Break,* vol 37, No 1, Jan. 2019, pp. 75-81.

Stopin, A., Plessix, R.-E., and S. Al Abri [2014]. Multiparameter waveform inversion of a large wide azimuth low-frequency land data set in Oman. *Geophysics*, **79**(3), WA67-WA77.

Tessmer, E., Kosloff, D. and Behle, A. [1992] Elastic wave propagation simulation in the presence of surface topography. *Geophys. J. Int.*, **108**, 621-632.

Tverdokhlebov, D., V. Korobkin, A. Kleshnin, E. Kashirina, E. Danko, V. Zaravnyaev, R. Melnikov [2018]. FWI as an effective solution for land near-surface model building into the area with complex geological settings: Eastern Siberia case study, *First Break*, **37**, 39-47.

Vigh, D., X. Cheng, K. Jiao, Z. Xu and D. Sun, 2018. Essential steps for successful full-waveform inversion using land data, SEG International Exposition and 88th annual Meeting, Extended abstract, 1128-1132.

Zhang, W. and Chen, X. [2006] Traction image method for irregular free surface boundaries in finite difference seismic wave simulation. *Geophys. J. Int.*, **167**, 337-353.

Zhang, Y., Zhang, H. and Zhang, G. [2011] A stable TTI reverse time migration and its implementation: *Geophysics*, **76**, WA3-WA11.